

Robust Deterministic Policy Gradient in Zero-Sum Games for Disturbance Attenuation

Taeho Lee¹ and Donghwan Lee^{1*}

¹*The School of Electrical Engineering, Korea Advanced Institute of Science and Technology, 291 Daehak-ro, Yuseong-gu, Daejeon, 34141, Republic of Korea.

*Corresponding author(s). E-mail(s): donghwan@kaist.ac.kr;
Contributing authors: eho0228@kaist.ac.kr;

Abstract

Practical control systems pose significant challenges in identifying optimal control policies due to uncertainties in the system model and external disturbances. While H_∞ control techniques are commonly used to design robust controllers that mitigate the effects of disturbances, these methods often require complex and computationally intensive calculations. To address this issue, this paper proposes a reinforcement learning algorithm called robust deterministic policy gradient (RDPG), which formulates the H_∞ control problem as a two-player zero-sum dynamic game. In this formulation, one player (the user) aims to minimize the cost, while the other player (the adversary) seeks to maximize it. We then employ deterministic policy gradient (DPG) and its deep reinforcement learning counterpart to train a robust control policy with effective disturbance attenuation. In particular, for practical implementation, we introduce an algorithm called robust deep deterministic policy gradient (RDDPG), which employs a deep neural network architecture and integrates techniques from the twin-delayed deep deterministic policy gradient (TD3) to enhance stability and learning efficiency. To evaluate the proposed algorithm, we implement it on an unmanned aerial vehicle (UAV) tasked with following a predefined path in a disturbance-prone environment. The experimental results demonstrate that the proposed method outperforms other control approaches in terms of robustness against disturbances, enabling precise real-time tracking of moving targets even under severe disturbance conditions.

Keywords: Deep reinforcement learning, Two players zero-sum game, Unmanned aerial vehicles

1 Introduction

In recent years, deep reinforcement learning (DRL) has shown remarkable success in finding optimal policies across various domains, including games [1, 2] and control tasks [3, 4]. In particular, various model-free DRL algorithms, such as, deep deterministic policy gradient (DDPG) [3], twin delayed DDPG (TD3) [5], soft actor-critic (SAC) [6], and proximal policy optimization (PPO) [7], have demonstrated the ability to generate effective control inputs without requiring explicit system models. However, a critical challenge arises from the discrepancy between the simulation environments used for training and the real-world environment [8–10]. Therefore, developing DRL policies that are robust to unseen disturbances is crucial for ensuring reliability in real-world applications. To address this challenge, in this paper, we introduce adversarial learning, where the agent is trained in the presence of disturbances. By exposing the policy to worst-case scenarios during training, the agent can improve its robustness and generalization to unseen environments.

In this paper, we present the so-called robust deterministic policy gradient (RDPG) algorithm which enhances the robustness of deterministic policy gradient (DPG) algorithm [11] from the concept of the H_∞ control and the two-player zero-sum dynamic game perspectives. The H_∞ control [12–14] method is a robust control technique that aims to design an optimal controller that minimizes the impact of disturbances on system performance. A well-established result in control theory shows that, under certain assumptions, the H_∞ control problem can be reformulated as a two-player zero-sum dynamic game, or equivalently, a min-max optimization problem [15]. In this game-theoretic formulation, the controller (first player) seeks to minimize a given cost function, while the adversary (second player) simultaneously tries to maximize it by injecting disturbances [15].

Building upon this theoretical foundation, we transform the H_∞ control problem into a two-player zero-sum dynamic game between the user (the controller) and the adversarial agent. We then propose a reinforcement learning approach based on the DPG method to simultaneously train both agents. Each agent learns its own policy: the user aims to minimize the objective function, while the adversary aims to maximize it. As a result of this zero-sum game framework, the user learns a control policy that is inherently robust against worst-case disturbances. Furthermore, we extend this idea to high-dimensional continuous control settings by incorporating it into a deep reinforcement learning framework. The resulting algorithm, named robust deep deterministic policy gradient (RDDPG), combines the core idea of RDPG with TD3 [5].

Additionally, we aim to develop a robust control strategy for quadrotors, a widely used unmanned aerial vehicle (UAV) in various applications. The ability to maintain robust control of quadrotors is particularly important in dynamic and uncertain environments, where tasks such as tracking moving targets or following predefined waypoints are required. We demonstrate that the proposed RDDPG method effectively determines optimal control inputs in the presence of external disturbances. Furthermore, it outperforms existing DRL-based control approaches by achieving lower cost under severe disturbance conditions.

In conclusion, the main contributions can be summarized as follows:

1. We propose the RDPG algorithm, which enhances robustness against external disturbances by integrating concepts from H_∞ control and two-player zero-sum dynamic games into the actor-critic framework.
2. We develop a novel deep reinforcement learning algorithm, named RDDPG, which integrates RDPG into the TD3 framework to enable scalable and robust learning in continuous control tasks.
3. We apply the proposed RDDPG algorithm to the robust tracking control of quadrotors and conduct comprehensive numerical simulations. The results demonstrate that RDDPG significantly outperforms several state-of-the-art DRL methods, including DDPG, SAC, and TD3.

2 Related works

The H_∞ control methods are effective in designing robust controllers against disturbances and have demonstrated satisfactory performance in nonlinear dynamic systems [14, 16–18]. However, these methods require precise model linearization and incur high computational costs due to the need to solve Hamilton-Jacobi-Isaacs (HJI) equations. To address these limitations, alternative approaches leverage deep reinforcement learning (DRL) to determine optimal control policies without the need for solving nonlinear HJI equations.

Recent efforts have extended the ideas of H_∞ control and two-player zero-sum games into the DRL framework to enhance robustness under various scenarios. For instance, Deshpande et al. [19] developed a robust DRL approach to bridge the gap between different environments for quadcopter control tasks. Their method primarily addresses model uncertainties rather than external disturbances by adopting an action-robust reinforcement learning framework [9], where an adversary injects noise directly into the agent’s actions to minimize the agent’s reward. In contrast, our method explicitly introduces external disturbances into the environment dynamics and formulates the learning process as a two-player zero-sum game between the agent and the adversary. By doing so, our approach enables the agent to learn a control policy that is robust to worst-case disturbance scenarios, rather than merely compensating for action-level noise. Long et al. [10] proposed a novel approach that models robust locomotion learning as an interaction between the locomotion policy and a learnable disturbance generator. The disturbance is conditioned on the robot’s state and produces appropriate external forces to facilitate policy learning. To address modeling errors and discrepancies between training and testing conditions, robust adversarial reinforcement learning (RARL) [8] was proposed. RARL trains the agent to perform effectively in the presence of a destabilizing adversary that applies disturbance forces to the system. The agent and the adversary are concurrently trained using the trust region policy optimization (TRPO) algorithm, with the agent learning to maximize the expected reward while the adversary learns to minimize it. Although the underlying concept is similar, their approach differs significantly from ours. Both methods adopt stochastic policy frameworks, such as PPO and TRPO, and they do not impose explicit constraints on the adversary, which may lead to the generation of excessively strong or unrealistic disturbances during training. In contrast, our method is based

on deterministic policy gradients and explicitly incorporates the H_∞ control perspective into a two-player zero-sum game formulation, enabling more stable and practical learning in continuous control tasks.

3 Preliminaries

3.1 H_∞ Control

Let us consider the discrete time nonlinear discrete-time system

$$\begin{aligned} x_{k+1} &= f(x_k, u_k, w_k, v_k) \\ y_k &= g(x_k, u_k, w_k) \end{aligned} \quad (1)$$

where $x_k \in \mathbb{R}^p$ is the state, $u_k \in \mathbb{R}^m$ is the control input, $w_k \in \mathbb{R}^n$ is the disturbance, and $v_k \in \mathbb{R}^l$ is the process noise at time step k . Using the state-feedback controller $u = \pi(x)$, the system can be reduced to the autonomous closed-loop system

$$\begin{aligned} x_{k+1} &= f(x_k, \pi(x_k), w_k, v_k) \\ y_k &= g(x_k, \pi(x_k), w_k) \end{aligned}$$

Assume that the initial state x_0 is determined by $x_0 \sim \rho(\cdot)$, where ρ is the initial state distribution. Defining the stochastic processes $\mathbf{w}_{0:\infty} := (w_0, w_1, \dots)$ and $\mathbf{y}_{0:\infty} := (y_0, y_1, \dots)$, the system can be seen as a stochastic mapping from $\mathbf{w}_{0:\infty}$ to $\mathbf{y}_{0:\infty}$ as follows: $\mathbf{y}_{0:\infty} \sim T_\pi(\cdot | \mathbf{w}_{0:\infty})$, where T_π is the conditional probability of $\mathbf{y}_{0:\infty}$ given $\mathbf{w}_{0:\infty}$. Moreover, defining the L^2 norm for the general stochastic process $\mathbf{z}_{0:\infty} := (z_0, z_1, \dots)$ by

$$\|\mathbf{z}_{0:\infty}\|_{L^2} := \sqrt{\sum_{k=0}^{\infty} \mathbb{E}[\|z_k\|_2^2]},$$

The H_∞ norm of the autonomous system is defined as

$$\|T_\pi\|_\infty := \sup_{\mathbf{w}_{0:\infty} \neq 0} \frac{\|\mathbf{y}_{0:\infty}\|_{L^2}}{\|\mathbf{w}_{0:\infty}\|_{L^2}} \quad (2)$$

The goal of H_∞ control is to design a control policy π that minimizes the H_∞ norm of the system T_π . However, minimizing $\|T_\pi\|_\infty$ directly is often difficult in practical implementations. Instead, we typically aim to find an acceptable $\eta > 0$ and a controller satisfying $\|T_\pi\|_\infty \leq \eta$, which is called suboptimal H_∞ control problem. Then, the H_∞ control problem can be approximated to the problem of finding a controller π that satisfies the constraint

$$\|T_\pi\|_\infty^2 = \sup_{\mathbf{w}_{0:\infty} \neq 0} \frac{\|\mathbf{y}_{0:\infty}\|_{L^2}^2}{\|\mathbf{w}_{0:\infty}\|_{L^2}^2} \leq \eta^2 \quad (3)$$

Defining

$$J^\pi := \sup_{\mathbf{w}_{0:\infty} \neq 0} \mathbb{E} \left[\sum_{k=0}^{\infty} (\|y_k\|_2^2 - \eta^2 \|w_k\|_2^2) \middle| \pi \right]$$

the problem can be equivalently written by finding a controller π satisfying $J^\pi \leq 0$. The problem can be solved by

$$\pi^* := \arg \min_{\pi} J^\pi.$$

3.2 Two-player zero-sum dynamic game perspective

According to [15], the suboptimal H_∞ control problem can be equivalently viewed as solving a zero-sum dynamic game under certain assumptions. In particular, we consider two decision making agents called the user and the adversary, respectively. They sequentially take control actions u_k (user) and w_k (adversary) to minimize and maximize cumulative discounted costs, respectively, of the form

$$\mathbb{E} \left[\sum_{k=0}^{\infty} \gamma^k c(x_k, u_k, w_k) \right]$$

where $\gamma \in (0, 1]$ is the discount factor, u_k is the control input of the user, and w_k is the control input of the adversary. The two agents have opposing objectives. The user's primary objective entails minimizing the costs, while the adversary strives to hinder the user's progress by maximizing the costs. There exist two categories of the two-player dynamic games, the alternating two-player dynamic game and simultaneous two-player dynamic game. In the alternating two-player dynamic game, two agents engaged in decision making take turns in selecting actions to maximize and minimize the cost, respectively. On the other hand, in the simultaneous two-player dynamic game, the two agents take actions simultaneously to maximize and minimize the cost. In this paper, we mainly focus on the simultaneous two-player dynamic game.

We consider the state-feedback deterministic control policy for each agent, defined as $\pi : \mathbb{R}^p \rightarrow \mathbb{R}^m$ for the user and $\mu : \mathbb{R}^p \rightarrow \mathbb{R}^n$ for the adversary

$$u = \pi(x) \in \mathbb{R}^m, \quad w = \mu(x) \in \mathbb{R}^n, \quad x \in \mathbb{R}^p$$

The corresponding cost function is defined as

$$J^{\pi, \mu} := \mathbb{E} \left[\sum_{k=0}^{\infty} \gamma^k c(x_k, u_k, w_k) \middle| \pi, \mu \right] \quad (4)$$

The goal of the dynamic game is to find a saddle-point pair of equilibrium policies (π, μ) (if exists) for which

$$J^{\pi^*, \mu} \leq J^{\pi^*, \mu^*} \leq J^{\pi, \mu^*}, \quad \forall \pi \in \Pi, \quad \forall \mu \in \mathcal{M}$$

where Π denotes the set of all admissible state-feedback policies for the user and M denotes the set of all admissible state-feedback policies for the adversary. The above relation equivalently means

$$\mu^* = \max_{\mu \in M} J^{\pi^*, \mu}, \quad \pi^* = \min_{\pi \in \Pi} J^{\pi, \mu^*}$$

By the min-max theorem, this also implies that

$$\max_{\mu \in M} \min_{\pi \in \Pi} J^{\pi, \mu} = \min_{\pi \in \Pi} \max_{\mu \in M} J^{\pi, \mu}$$

The optimal cost is now defined as

$$J^* := J^{\pi^*, \mu^*}$$

To show a connection between the dynamic game framework and the H_∞ control problem, let us consider the specific per-step cost function

$$c(x, u, w) = \|g(x, u, w)\|_2^2 - \eta^2 \|w\|_2^2.$$

Then the corresponding cost function is then written when $\gamma = 1$ as

$$J^{\pi, \mu} = \mathbb{E} \left[\sum_{k=0}^{\infty} (\|y_k\|_2^2 - \eta^2 \|w_k\|_2^2) \middle| \pi, \mu \right]$$

The user's optimal policy is

$$\pi^* := \arg \min_{\pi \in \Pi} \max_{\mu \in M} J^{\pi, \mu}$$

which is structurally very similar to the policy with the H_∞ performance in the previous subsection. It is known that under some special conditions such as the linearity, the H_∞ suboptimal control policy and the saddle-point policy are equivalent when $J^* \leq 0$.

3.3 Bellman equations

Let us define the value function

$$V^{\pi, \mu}(x) := \mathbb{E} \left[\sum_{k=t}^{\infty} \gamma^k c(x_k, u_k, w_k) \middle| \pi, \mu, x_t = x \right]$$

so that the corresponding cost function is $J^{\pi, \mu} = \mathbb{E}[V^{\pi, \mu}(x) | x \sim \rho(\cdot)]$. We can also prove that the value function satisfies the Bellman equation

$$V^{\pi, \mu}(x) = c(x, \pi(x), \mu(x)) + \gamma \mathbb{E}[V^{\pi, \mu}(x') | \pi, \mu]$$

where x' implies the next state given the current state x and the action taken by (π, μ) . Let us define the optimal value function as $V^* := V^{\pi^*, \mu^*}$. Then, the corresponding optimal Bellman equation can be obtained by replacing (π, μ) by (π^*, μ^*) . Similarly, let us define the so-called Q-function by

$$Q^{\pi, \mu}(x, u, w) := \mathbb{E} \left[\sum_{k=t}^{\infty} \gamma^k c(x_k, u_k, w_k) \middle| x_t = x, u_t = u, w_t = w, \pi, \mu \right]$$

which satisfies the Q-Bellman equation

$$Q^{\pi, \mu}(x, u, w) = c(x, u, w) + \gamma \mathbb{E}[Q^{\pi, \mu}(x', u', w') | \pi, \mu]$$

where x' implies the next state given the current state x and action pair (u, w) , u' means the next action of the user given x' and under π , and w' implies the next action of the adversary given x' and under μ . Defining the optimal Q-function $Q^* := Q^{\pi^*, \mu^*}$, one can easily prove the optimal Q-Bellman equation

$$Q^*(x, u, w) = c(x, u, w) + \gamma \mathbb{E}[Q^*(x', u', w') | \pi^*, \mu^*]$$

4 Proposed method

In this section, we will present the proposed method, robust deterministic policy gradient (RDPG) and its deep reinforcement learning version, robust deep deterministic policy gradient (RDDPG).

Figure 1 illustrates the architecture of the proposed method, RDDPG, based on a two-player zero-sum dynamic game. In this method, two policy, user policy π and adversary policy μ , interact within the environment. The user policy generates the action u_t , while the adversary policy generates the disturbance w_t , both based on the current state x_t . These inputs are fed into the environment, which returns the next state x_{t+1} and the cost c_t based on the dynamics of the environment. The critic is updated based on $\{x_t, u_t, w_t, x_{t+1}, c_t\}$ and evaluates the joint performance of the user and adversary. The policy of user and adversary are updated by deterministic policy gradient method to minimize and maximize the objective function $J^{\pi, \mu}$. The detailed procedure is described in the following sections.

4.1 Robust deterministic policy gradient

To apply deterministic policy gradient (DPG) [11] to the two-player zero-sum dynamic games, we consider the parameterized deterministic control policies

$$u = \pi_\theta(x) \in \mathbb{R}^m, \quad w = \mu_\phi(x) \in \mathbb{R}^n, \quad x \in \mathbb{R}^p$$

where $\pi_\theta : \mathbb{R}^p \rightarrow \mathbb{R}^m$ denotes the user's control policy parameterized by θ and $\mu_\phi : \mathbb{R}^p \rightarrow \mathbb{R}^n$ denotes the adversary's control policy parameterized by ϕ . The saddle-point

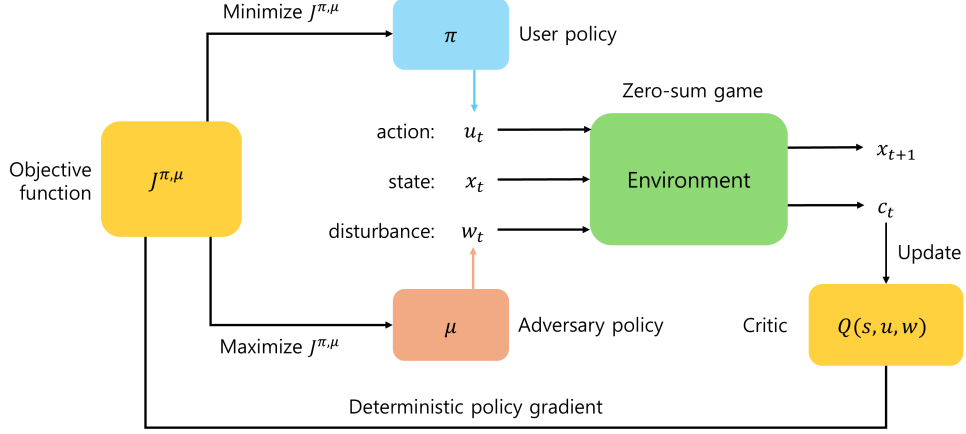


Fig. 1 Overview of RDDPG. Based on the two-player zero-sum dynamic game, the user policy π seeks to minimize the objective function $J^{\pi, \mu}$, while the adversary policy μ attempts to maximize it by injecting disturbances into the environment.

problem is then converted to

$$\theta^* := \arg \min_{\theta} \max_{\phi} J^{\pi_{\theta}, \mu_{\phi}}$$

which can be solved using the primal-dual iteration

$$\begin{aligned} \theta_{k+1} &= \theta_k - \alpha_{\theta} \nabla_{\theta} J^{\pi_{\theta}, \mu_{\phi_k}} \Big|_{\theta=\theta_k}, \\ \phi_{k+1} &= \phi_k + \alpha_{\phi} \nabla_{\phi} J^{\pi_{\theta_{k+1}}, \mu_{\phi}} \Big|_{\phi=\phi_k} \end{aligned}$$

where $\alpha_{\theta} > 0$ and $\alpha_{\phi} > 0$ are step-sizes. According to [11], the deterministic gradients can be obtained using the following theorem.

Theorem 1 *The deterministic policy gradients for the user and adversary policies are given by*

$$\nabla_{\theta} J^{\pi_{\theta}, \mu_{\phi}} = \mathbb{E} \left[\nabla_{\theta} Q^{\pi_{\theta}, \mu_{\phi}}(s, \pi_{\theta}, \mu_{\phi}) \Big|_{\pi=\pi_{\theta}} \middle| s \sim \rho \right]$$

and

$$\nabla_{\phi} J^{\pi_{\theta}, \mu_{\phi}} = \mathbb{E} \left[\nabla_{\phi} Q^{\pi_{\theta}, \mu}(s, \pi_{\theta}, \mu_{\phi}) \Big|_{\mu=\mu_{\phi}} \middle| s \sim \rho \right]$$

respectively.

The proof is a simple extension of the DPG theorem in [11], so it is omitted here. A reinforcement learning counterpart to DPG can be obtained by using the samples

of the gradients. Next, we will consider the following per-step cost function:

$$c(x, u, w) = \tilde{c}(x, u, w) - \eta^2 \|w\|_2^2$$

where $\tilde{c} : \mathbb{R}^p \times \mathbb{R}^m \times \mathbb{R}^n \times \mathbb{R}^p \rightarrow \mathbb{R}$ is the cost function for the user. Note that the cost function \tilde{c} can be set arbitrarily and is more general than the quadratic cost in the H_∞ control problem. This is because the H_∞ control problem can be recovered by setting

$$\tilde{c}(x, u, w) = \|g(x, u, w, v)\|_2^2$$

In this way, we can consider the two-player zero-sum dynamic game as an extension of the usual reinforcement learning tasks by considering robustness against the adversarial disturbance. The additional disturbance quadratic cost $\eta^2 w^T w$ in the cost function discourages the adversary from generating excessively large disturbances, effectively regularizing its behavior and ensuring that the learned policies are robust against realistic worst-case scenarios rather than arbitrary or unbounded inputs.

Let us assume that we found some approximate solutions $\theta_\epsilon^*, \phi_\epsilon^*$ such that $J^{\pi_{\theta_\epsilon^*}, \mu_{\phi_\epsilon^*}} \leq 0$. Then, this implies that

$$\frac{\mathbb{E} \left[\sum_{k=0}^{\infty} \gamma^k \tilde{c}(x_k, u_k, w_k) \middle| \pi_{\theta_\epsilon^*}, \mu_{\phi_\epsilon^*} \right]}{\mathbb{E} \left[\sum_{k=0}^{\infty} \gamma^k \|w_k\|_2^2 \middle| \pi_{\theta_\epsilon^*}, \mu_{\phi_\epsilon^*} \right]} \leq \eta^2$$

4.2 Robust deep deterministic policy gradient

To implement RDPG in high-dimensional continuous control tasks, we incorporate the techniques from twin-delayed deep deterministic policy gradient (TD3)[\[5\]](#), resulting in the RDPG. In particular, we introduce the following networks:

1. The online actor network π_θ for the user and the online actor network μ_ϕ for the adversary
2. The corresponding target networks $\pi_{\theta'}$, $\mu_{\phi'}$ for the two online actor network
3. Two online critic networks $Q_{\psi_1}(x, u, w)$, $Q_{\psi_2}(x, u, w)$
4. The corresponding target networks $Q_{\psi'_1}(x, u, w)$, $Q_{\psi'_2}(x, u, w)$

Now, following [\[5\]](#), the actor and critic networks are trained through the following procedures.

4.2.1 Critic update

The critic is trained by the gradient descent step to the loss

$$L_{\text{critic}}(\psi_i; B) := \frac{1}{|B|} \sum_{(x, u, w, c, x') \in B} (y - Q_{\psi_i}(x, u, w))^2, \quad i \in \{1, 2\}$$

where B is the mini-batch, $|B|$ is the size of the mini-batch, c is the cost incurred at the same time as the state x , and x' means the next state. Moreover, the target y is

defined as

$$y = c + \gamma \max_{i \in \{1, 2\}} Q_{\psi'_i}(x', \tilde{u}, \tilde{w})$$

when x' is not the terminal state, and

$$y = c$$

when x' is the terminal state (in the episodic environments), where

$$\begin{aligned}\tilde{u} &= \pi_{\theta'}(x') + \text{clip}(\epsilon_1, -\delta, \delta) \quad \epsilon_1 \sim \mathcal{N}(0, \sigma) \\ \tilde{w} &= \mu_{\phi'}(x') + \text{clip}(\epsilon_2, -\delta, \delta) \quad \epsilon_2 \sim \mathcal{N}(0, \sigma)\end{aligned}$$

where ϵ_1, ϵ_2 are random noise vectors added in order to smooth out the target values, $\mathcal{N}(0, \sigma)$ implies the Gaussian distribution with zero mean and variance σ , and the clip function is added in order to guarantee the boundedness of the control inputs. The critic's online parameters ψ_1, ψ_2 are updated by the gradient descent step to minimize the loss

$$\psi_i \leftarrow \psi_i - \alpha_{\text{critic}} \nabla_{\psi_i} L_{\text{critic}}(\psi_i; B), \quad i \in \{1, 2\}$$

where α_{critic} is the step-size. After the online critics are updated, the target parameters of two critic ψ'_1 and ψ'_2 are updated as follows:

$$\psi'_i \leftarrow \tau \psi_i + (1 - \tau) \psi'_i, \quad i \in \{1, 2\}$$

where $\tau \in (0, 1)$ serves as the interpolation coefficient, facilitating a gradual update that enhances training stability.

4.2.2 Actor update

The actor networks for the user and adversary are updated using the sampled deterministic policy gradient

$$\begin{aligned}\theta &\leftarrow \theta - \alpha_{\text{actor}} \nabla_{\theta} L_{\text{actor}}(\theta, \phi; B) \\ \phi &\leftarrow \phi + \beta_{\text{actor}} \nabla_{\phi} L_{\text{actor}}(\theta, \phi; B)\end{aligned}$$

where α_{actor} and β_{actor} are the step-sizes, and

$$L_{\text{actor}}(\theta, \phi; B) = \frac{1}{|B|} \sum_{(x, u, w, r, x') \in B} Q_{\psi_1}(x, \pi_{\theta}(x), \mu_{\phi}(x))$$

Please note the opposite signs of the gradients for the user and adversary updates, which are due to their opposite roles. After the online actors are updated, the target parameters of actor θ' and ϕ' are updated as follows

$$\theta' \leftarrow \tau \theta + (1 - \tau) \theta', \quad \phi' \leftarrow \tau \phi + (1 - \tau) \phi'$$

where $\tau \in (0, 1)$ is the interpolation coefficient.

Algorithm 1 RDDPG

- 1: Initialize the online critic networks Q_{ψ_1}, Q_{ψ_2}
- 2: Initialize the actor networks π_θ, μ_ϕ for the user and adversary, respectively.
- 3: Initialize the target parameters $\psi'_1 \leftarrow \psi_1, \psi'_2 \leftarrow \psi_2, \theta' \leftarrow \theta, \phi' \leftarrow \phi$
- 4: Initialize the replay buffer \mathcal{D}
- 5: **for** Episode $i=1,2,\dots N_{iter}$ **do**
- 6: Observe s_0
- 7: **for** Time step $k=0,1,2,\dots \tau-1$ **do**
- 8: Select actions $u_k = \pi_\theta(x_k) + e_1$ and $w_k = \mu_\phi(x_k) + e_2$,
where $e_1, e_2 \sim \mathcal{N}(0, \sigma)$ are exploration noises.
- 9: Compute the cost $c_{k+1} := c(x_k, u_k, w_k)$
- 10: Observe the next state x_{k+1}
- 11: Store the transition tuple $(x_k, u_k, w_k, c_{k+1}, x_{k+1})$ in the replay buffer \mathcal{D}
- 12: Uniformly sample a mini-batch B from the replay buffer \mathcal{D}
- 13: Update critic network:

$$\psi_i \leftarrow \psi_i - \alpha_{\text{critic}} L_{\text{critic}}(\psi_i; B), \quad i \in \{1, 2\}$$

- 14: Update actor networks by the deterministic policy gradient:

$$\begin{aligned} \theta &\leftarrow \theta - \alpha_{\text{actor}} \nabla_\theta L_{\text{actor}}(\theta, \phi; B) \\ \phi &\leftarrow \phi + \beta_{\text{actor}} \nabla_\phi L_{\text{actor}}(\theta, \phi; B) \end{aligned}$$

- 15: Update actor networks by the deterministic policy gradient:
- 16: Soft update target networks:

$$\begin{aligned} \theta' &\leftarrow \tau\theta + (1 - \tau)\theta' \\ \phi'_i &\leftarrow \tau\phi + (1 - \tau)\phi' \end{aligned}$$

- 17: **end for**
- 18: **end for**

4.2.3 Exploration

For exploration during training, Gaussian noise is added to both the user's control action and the adversary's disturbance. Specifically, the user's action u_k and the adversary's disturbance w_k at time step k are expressed as

$$\begin{aligned} u_k &= \pi_\theta(x_k) + e_1 \\ w_k &= \mu_\phi(x_k) + e_2 \end{aligned}$$

where $e_1, e_2 \sim \mathcal{N}(0, \sigma)$ represent zero-mean Gaussian exploration noises with standard deviation σ [5]. The overall algorithm is summarized in Algorithm 1.

5 Quadrotor application

5.1 Quadrotor dynamics model

The quadrotor dynamics can be described as follows:

$$m\mathbf{a}_k = m \begin{bmatrix} 0 \\ 0 \\ -g \end{bmatrix} + \mathbf{R}\mathbf{T}_k + \mathbf{F}_D + w_k \quad (5)$$

$$\Delta\omega_k = I^{-1}(-\omega_{k-1} \times I\omega_{k-1} + \tau_B) \quad (6)$$

$$\mathbf{v}_k = \mathbf{v}_{k-1} + T_s \mathbf{a}_k \quad (7)$$

$$\mathbf{p}_k = \mathbf{p}_{k-1} + T_s \mathbf{v}_k \quad (8)$$

$$\omega_k = \omega_{k-1} + T_s \Delta\omega_k \quad (9)$$

$$\rho_k = \rho_{k-1} + T_s \omega_k \quad (10)$$

where m is the mass of the quadrotor, g is the gravity acceleration, T_s is the sampling time, $w_k = [w_{k,x}, w_{k,y}, w_{k,z}]^T$ means an external disturbance applied to the quadrotor, $\mathbf{a}_k = [a_{k,x}, a_{k,y}, a_{k,z}]^T$ denotes linear acceleration, $\mathbf{v}_k = [v_{k,x}, v_{k,y}, v_{k,z}]^T$ represents linear velocity, $\mathbf{p}_k = [p_{k,x}, p_{k,y}, p_{k,z}]^T$ describes the position of the quadrotor in the inertial frame, $\Delta\omega_k = [\Delta\omega_{k,\phi}, \Delta\omega_{k,\theta}, \Delta\omega_{k,\psi}]^T$ is angular acceleration, $\omega_k = [\omega_{k,\phi}, \omega_{k,\theta}, \omega_{k,\psi}]^T$ is the angular velocity, and $\rho_k = [\phi_k, \theta_k, \psi_k]^T$ represents the roll, pitch, yaw of the quadrotor in the body frame. Moreover, \mathbf{R} is the rotation matrix from the body frame to the inertial frame, and \mathbf{T}_B is the total thrust of the quadrotor along the z axis in the body frame and defined as follows:

$$\mathbf{T}_k = \sum_{i=1}^4 T_{k,i} = k_F \begin{bmatrix} 0 \\ 0 \\ \sum \text{RPM}_{k,i}^2 \end{bmatrix}$$

where $T_{k,i}$ is the thrust generated by i th motor, k_F is the thrust coefficient, and $\text{RPM}_{k,i}$ is the speed of i th motor at time step k . \mathbf{F}_D is a drag force, which is generated by motor spinning, defined as

$$\mathbf{F}_D = -\mathbf{K}_D \left(\sum_{i=1}^4 \text{RPM}_{k,i} \right) \mathbf{v}_k$$

where $\mathbf{K}_D = \text{diag}(K_{D,x}, K_{D,y}, K_{D,z})$ is a matrix of drag coefficients. Among the four motors, two opposing motors (1st and 3rd) rotate clockwise, while the others (2nd and 4th) rotate counterclockwise. This causes torque τ_k in the roll, pitch, yaw directions

$$\tau_k = \begin{bmatrix} \tau_{k,\phi} \\ \tau_{k,\theta} \\ \tau_{k,\psi} \end{bmatrix} = \begin{bmatrix} l' k_F (\text{RPM}_{k,2}^2 - \text{RPM}_{k,4}^2) \\ l' k_F (-\text{RPM}_{k,1}^2 + \text{RPM}_{k,3}^2) \\ k_M (\text{RPM}_{k,1}^2 - \text{RPM}_{k,2}^2 + \text{RPM}_{k,3}^2 - \text{RPM}_{k,4}^2) \end{bmatrix}$$

where $l' = \cos(\frac{\pi}{4})l$ is the scaled arm length, because the motors of the quadrotor are positioned at a 45-degree angle relative to the x and y axes when the yaw angle is 0, k_F is the thrust coefficient, and k_M is the torque coefficient. The inertia matrix, denoted by the symbol I , represents the inertial properties of the quadrotor's body.

5.2 State space

The state x_k of the quadrotor is defined as

$$x_k = [\mathbf{e}_k^p, \mathbf{e}_k^v, \boldsymbol{\rho}_k, \boldsymbol{\omega}_k]^T \in \mathbb{R}^{12}$$

where \mathbf{e}_k^p denotes the position error, \mathbf{e}_k^v represents the velocity error, $\boldsymbol{\rho}_k$ is the Euler angle vector, and $\boldsymbol{\omega}_k$ is the angular velocity vector. These quantities are defined as follows:

$$\begin{aligned} \mathbf{e}_k^p &= \mathbf{p}_k^{\text{target}} - \mathbf{p}_k \\ &= [p_{k,x}^{\text{target}} - p_{k,x}, p_{k,y}^{\text{target}} - p_{k,y}, p_{k,z}^{\text{target}} - p_{k,z}]^T \in \mathbb{R}^3 \\ \mathbf{e}_k^v &= \mathbf{v}_k^{\text{target}} - \mathbf{v}_k \\ &= [v_{k,x}^{\text{target}} - v_{k,x}, v_{k,y}^{\text{target}} - v_{k,y}, v_{k,z}^{\text{target}} - v_{k,z}]^T \in \mathbb{R}^3 \\ \boldsymbol{\rho}_k &= [\phi_k, \theta_k, \psi_k]^T \in \mathbb{R}^3 \\ \boldsymbol{\omega}_k &= [\omega_{k,\phi}, \omega_{k,\theta}, \omega_{k,\psi}]^T \in \mathbb{R}^3 \end{aligned}$$

where $\mathbf{p}_k^{\text{target}}$ and \mathbf{p}_k denote the position vectors of the target and the quadrotor, respectively, and $\mathbf{v}_k^{\text{target}}$ and \mathbf{v}_k represent their corresponding linear velocity vectors. ϕ_k, θ_k, ψ_k denotes roll, pitch, yaw of the quadrotor. As in the method used in deep Q-network (DQN) [2], we used the last four time steps of the state as input to the neural network to help the network better capture dynamics in the environment.

5.3 Action space

The action of the quadrotor, u_k , is the speed of four motors $\text{RPM}_{k,i}$, $i \in \{1, 2, 3, 4\}$, which is continuous value between 0 and 21713.714, as follows:

$$u_k := [\text{RPM}_{k,1}, \text{RPM}_{k,2}, \text{RPM}_{k,3}, \text{RPM}_{k,4}]^T \in \mathbb{R}^4.$$

The action of the disturbance adversary, w_k , represents the external forces to the quadrotor along the x , y , and z axes of the body frame as follows:

$$w_k := [w_{k,x}, w_{k,y}, w_{k,z}]^T \in \mathbb{R}^3$$

5.4 Cost function

The cost function $c(x_k, u_k, w_k)$ is comprised of the cost function for the user $\tilde{c}(x_k, u_k)$ and the disturbance quadratic cost $\eta^2 w_k^T w_k$. The cost function for the user $\tilde{c}(x_k, u_k)$ is the sum of the following terms: $\tilde{c}(x_k, u_k) = c_{k,p} + c_{k,v} + c_{k,\rho} + c_l + c_{tr}$

1. Position error cost $c_{k,p}$: Position error between the target and quadrotor

$$c_{k,p} = \alpha \times \|\mathbf{e}_k^p\|_2^2$$

2. Velocity error cost $c_{k,v}$: Velocity error between the target and quadrotor

$$c_{k,v} = \beta \times \|\mathbf{e}_k^v\|_2^2$$

3. Angle cost $c_{k,\rho}$: Magnitude of roll, pitch, and yaw of the quadrotor

$$c_{k,\rho} = \epsilon \times \|\boldsymbol{\rho}_k\|_2^2$$

4. Living cost c_l : Constant cost at every step

$$c_l = \lambda$$

5. Penalty cost c_{tr} : Penalty when the quadrotor fails to track the target

$$c_{tr} = \begin{cases} \zeta & \text{if } \|\mathbf{e}_k^p\|_2 \geq 5 \text{ or } \phi_k, \theta_k \geq \frac{\pi}{2} \\ 0 & \text{else} \end{cases}$$

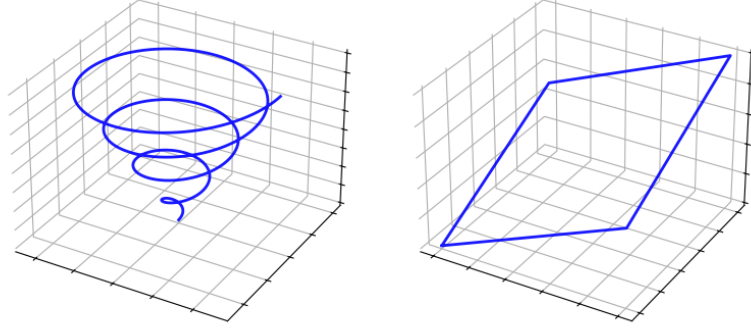
where the scaling factors α , β , ϵ , and ζ are positive (i.e., $\alpha, \beta, \epsilon, \zeta > 0$), and λ is negative (i.e., $\lambda < 0$). The specific values used for these parameters are summarized in the Appendix A2. Since α and β are positive, the quadrotor agent learns a policy that minimizes position and velocity errors. If the quadrotor's angles become too large, it becomes more susceptible to disturbances and may flip easily. Therefore, minimizing the angles cost c_ρ is crucial for stability. Additionally, the living cost c_l is a negative reward that encourages the quadrotor to maintain stability. The penalty cost c_{tr} is a large positive value applied when the quadrotor fails to track the target—specifically, when the distance between the target and the quadrotor exceeds 5 meters, or when the quadrotor flips with roll or pitch angles exceeding $\frac{\pi}{2}$. The agent learns a policy to avoid receiving this penalty, which can accelerate the initial learning process.

6 Experiments and results

6.1 Experiments setups

For experiments, we used the gym-pybullet-drones environment [20], which is an open-source quadrotor simulator built with Python and the Bullet Physics engine. This environment provided a modular and precise physics implementation, supporting both low-level and high-level control. In the simulator, the Crazyflie 2.0 quadrotor was modeled, and its parameters were summarized in Appendix Table A1.

To demonstrate the robustness of the proposed RDDPG algorithm, we compared it with other model-free reinforcement learning algorithms, including DDPG [3], TD3 [5], and SAC [6]. These methods utilized a single agent that aimed to minimize the cost function \tilde{c} . To enhance their robustness against disturbances, random external



Traj (1)

Traj (2)

Fig. 2 Two evaluation trajectories, denoted as Traj (1) and Traj (2), shown from left to right.

disturbances were applied during the training process. A detailed summary of the hyperparameters used in training was provided in Appendix [A3](#) and [A4](#).

For evaluation, we generated two trajectories as shown in Fig. 2. During evaluation, we introduced random wind disturbances in the x and y directions. We considered three scenarios where the maximum wind velocity was limited to ± 5 , ± 10 , and ± 15 [m/s], which were referred to as the ± 5 , ± 10 , and ± 15 wind speed scenarios in the figures and tables. In each scenario, the initial wind speed was randomly set within a given range and updated every 10 time steps with normally distributed noise.

Each algorithm was tested over 500 episodes and evaluated based on the mean and standard deviation of the total cost per episode, where the total cost was computed as the sum of the per-step costs $\tilde{c}(x_k, u_k)$ over a single episode. In addition, the mean and standard deviation of the position error $\|\mathbf{e}_k^p\|_2^2$ between the target and the quadrotor at each timestep were also considered as evaluation metrics.

6.2 Results

Figure 3 presents the mean and standard deviation of the total cost sum per episode under varying wind disturbance situation(± 5 , 10 , and 15) and across two distinct trajectories. Across all scenarios, RDDPG consistently achieves the lowest total cost sum, indicating its superior robustness compared to other DRL algorithms. As the magnitude of wind speed increases, the performance gap between RDDPG and other algorithms becomes more pronounced. Notably, TD3, which is the baseline algorithm of RDDPG, exhibits significant performance degradation with its mean cost increasing sharply and variance widening, especially in the ± 10 and ± 15 wind conditions. This suggests that TD3 is vulnerable to strong disturbances, even though it was trained under disturbed environments, as it failed to learn robust policies to such perturbations. DDPG and SAC both demonstrate relatively stable performance under mild disturbances, but they struggle significantly as wind strength increases. DDPG exhibits slightly lower average tracking errors in some cases, but its higher total

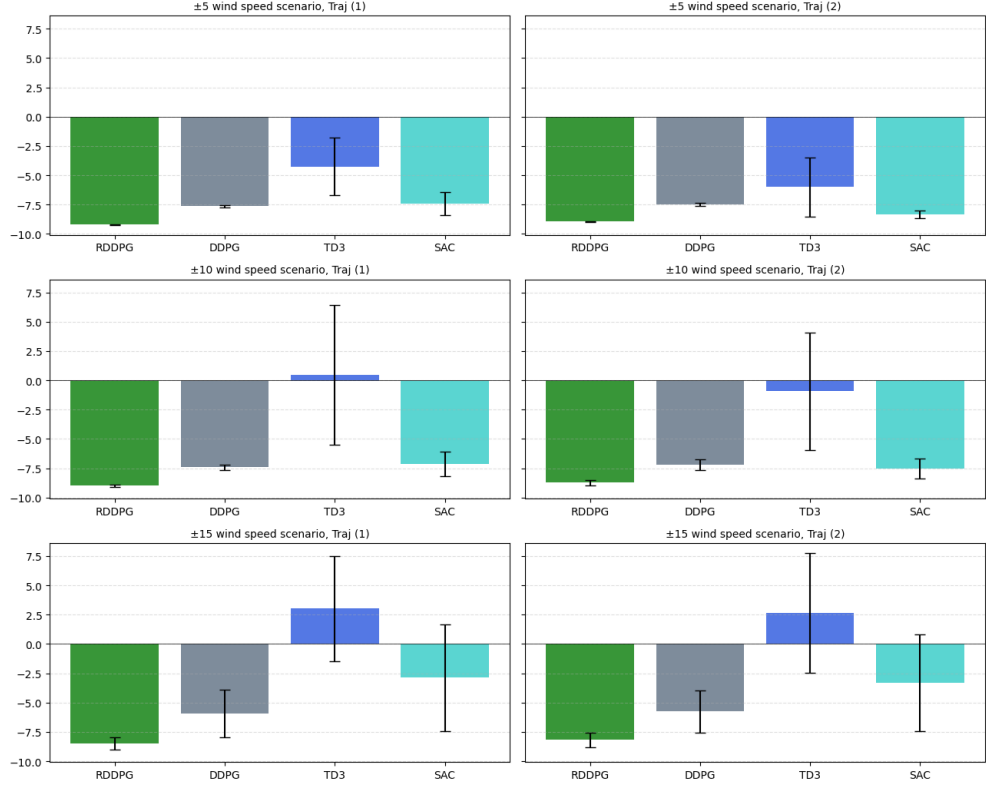


Fig. 3 Mean and standard deviation of the total episode cost. RDDPG achieves the lowest average cost and the smallest variance across all scenarios. This indicates that the RDDPG yields a robust agent that performs consistently even under severe external disturbances.

cost indicates that the quadrotor suffers from severe angular deviations and oscillatory behaviors, particularly under high-wind conditions. SAC, while stable under low-wind scenarios, fails to adapt effectively as disturbances grow stronger. Together, these results imply that neither DDPG nor SAC can reliably handle strong external disturbances, limiting their applicability in real-world scenarios.

By maintaining a consistently low and stable cost across a wide range of disturbance intensities, RDDPG exhibits superior robustness and reliable control performance, even under challenging environmental conditions. This enhanced robustness stems from its adversarial training framework, inspired by H_∞ control theory and formulated as a two-player zero-sum game. By optimizing the policy against worst-case disturbances during training, RDDPG learns disturbance-resilient strategies that improve generalization and ensure stable performance under unseen or highly uncertain conditions.

Figure 4 illustrates the trajectory tracking performance of each algorithm across varying wind speeds. RDDPG achieves the most accurate trajectory tracking, exhibiting the smallest tracking error compared to the other algorithms. The mean and

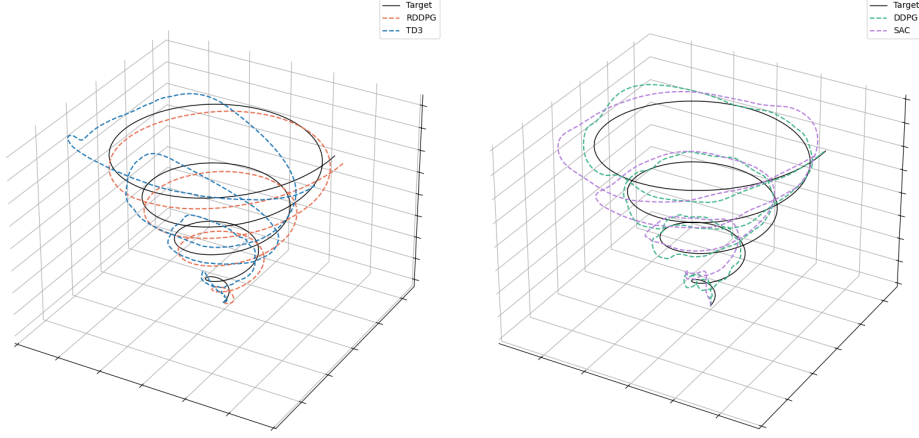


Fig. 4 Trajectory results of all algorithms under the ± 15 wind scenario and Traj (1).

standard deviation of the position error $\|\mathbf{e}_k^p\|_2^2$ between the target and the quadrotor is presented in Figure 5. Across all scenarios, RDDPG consistently achieves lower position errors compared to TD3 and SAC. In the case of DDPG, it exhibits lower position errors under mild wind disturbance scenarios. However, as the disturbance becomes stronger, its performance degrades significantly, resulting in higher errors compared to RDDPG. Furthermore, DDPG shows larger standard deviations, indicating less stable performance across episodes. Detailed numerical results are provided in at Appendix Table B5.

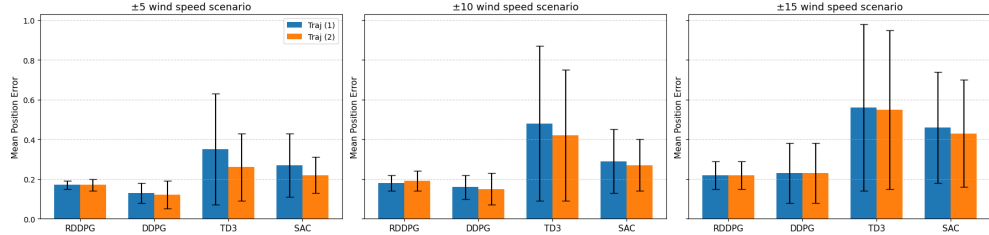


Fig. 5 Mean and standard deviation of the position error $\|\mathbf{e}_k^p\|_2^2$ between the target and the quadrotor at each time step. RDDPG consistently achieves low error and standard deviation across all scenarios, whereas other methods exhibit unstable performance.

7 Conclusion

This paper proposes RDPG, which combines the concept of the H_∞ control problem and a two-player zero-sum dynamic game framework, to overcome the robustness problem of DRL algorithms. In RDPG, the user seeks to minimize the cost function

while the adversary attempts to maximize it, thereby enabling the agent to learn a control policy that is robust to external disturbances. Furthermore, we introduce RDDOG, which integrates the robustness framework of RDPG with the learning stability of TD3, achieving both improved disturbance resistance and efficient policy learning in continuous control tasks. In order to evaluate the robustness of RDPG, we implement it on quadrotor tracking tasks under various external disturbances. Experimental results show that RDPG successfully learns an optimal control policy while maintaining stable performance across different disturbance scenarios. These findings demonstrate that RDPG outperforms other DRL-based methods in terms of robustness and reliability in real-world-inspired environments.

Appendix A Hyperparameters Used in Training

A.1 Physical parameters of Crazyflies 2.0

Table A1 Physical parameters of the Crazyfile 2.0

Parameter	Description	Value
m	Total mass	$0.027[\text{kg}]$
l	Arm length	$0.0397[\text{m}]$
K_F	Thrust coefficient	3.16×10^{-10}
K_M	Torque coefficient	7.94×10^{-12}
I_{xx}	Principal Moment of Inertia around x axis	$1.4 \times 10^{-3} [\text{kg} \times \text{m}^2]$
I_{yy}	Principal Moment of Inertia around y axis	$1.4 \times 10^{-3} [\text{kg} \times \text{m}^2]$
I_{zz}	Principal Moment of Inertia around z axis	$2.17 \times 10^{-3} [\text{kg} \times \text{m}^2]$
$K_{D,xy}$	Drag coefficients in x, y axes	9.18×10^{-7}
$K_{D,z}$	Drag coefficients in z axis	10.31×10^{-7}

A.2 Cost function

Table A2 Scaling factors in cost function

Parameter	Description	Value
α	Coefficient for position error	10
β	Coefficient for velocity error	1
ϵ	Coefficient for angle error	1
λ	Living reward	-10
ζ	Penalty	1000

A.3 DDPG and TD3

Table A3 Caption

Parameter	Description	Value
α_{actor}	Learning rate for user	0.0001
β_{actor}	Learning rate for adversary	0.0001
α_{critic}	Learning rate for critic	0.001
$ B $	Batch size	256
γ	Discounted factor	0.99
σ	Exploration noise	0.2

A.4 SAC

Table A4 SAC hyper-parameters

Parameter	Description	Value
α_{actor}	Learning rate for user	0.0003
α_{critic}	Learning rate for critic	0.003
$ B $	Batch size	256
γ	Discounted factor	0.99
$\alpha_{entropy}$	Entropy coefficient	0.99

Appendix B Experiment results

Table B5 The mean and standard deviation of the position error $\|\mathbf{e}_k^p\|_2$ between the target and the quadrotor. Bold indicates the best performance algorithm

	± 5 wind speed		± 10 wind speed		± 15 wind speed	
	Traj (1)	Traj (2)	Traj (1)	Traj (2)	Traj (1)	Traj (2)
RDDPG	0.17 ± 0.02	0.17 ± 0.03	0.18 ± 0.04	0.19 ± 0.05	0.22 ± 0.07	0.22 ± 0.07
DDPG	0.13 ± 0.05	0.12 ± 0.07	0.16 ± 0.06	0.15 ± 0.08	0.23 ± 0.15	0.23 ± 0.15
TD3	0.35 ± 0.28	0.26 ± 0.17	0.48 ± 0.39	0.42 ± 0.33	0.56 ± 0.42	0.55 ± 0.40
SAC	0.27 ± 0.16	0.22 ± 0.09	0.29 ± 0.16	0.27 ± 0.13	0.46 ± 0.28	0.43 ± 0.27

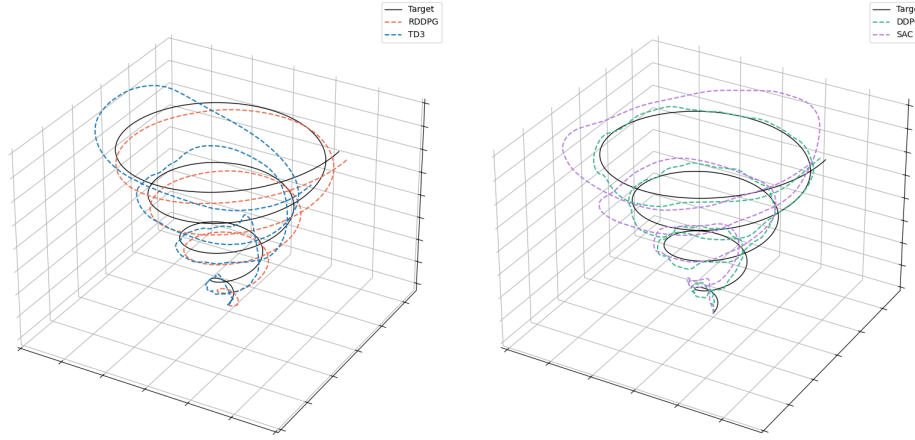


Fig. B1 In ± 15 m/s wind scenario

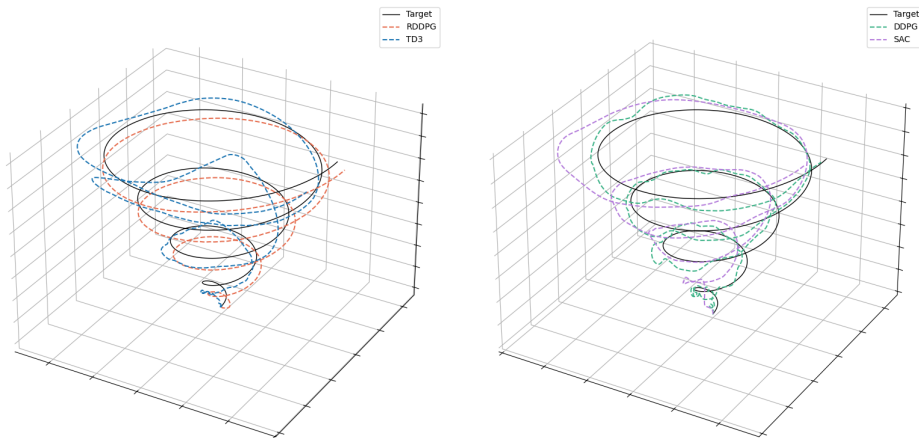


Fig. B2 In ± 15 m/s wind scenario

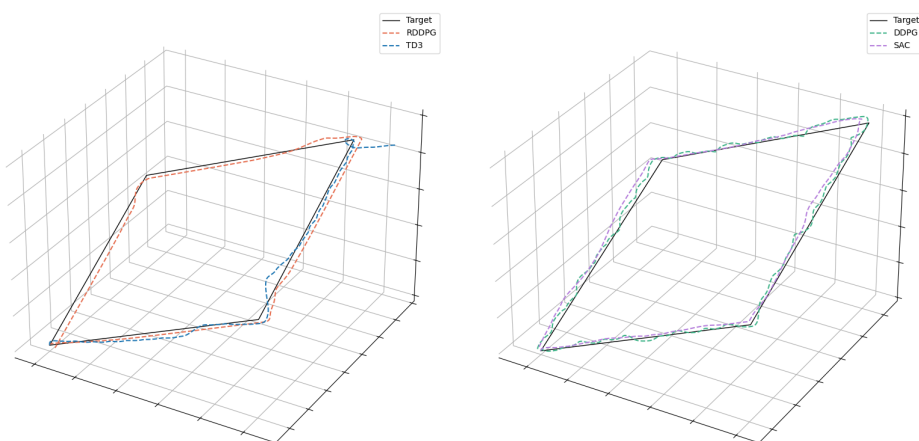


Fig. B3 In ± 15 m/s wind scenario

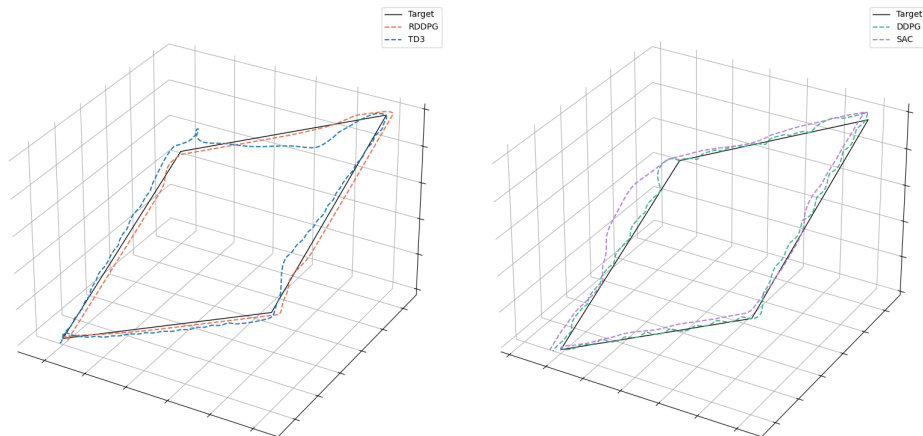


Fig. B4 In ± 15 m/s wind scenario

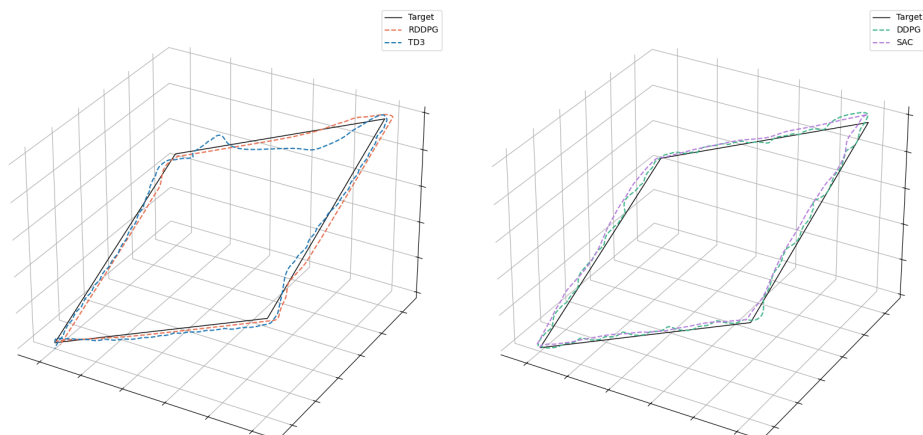


Fig. B5 In ± 15 m/s wind scenario

References

- [1] Silver, D., Schrittwieser, J., Simonyan, K., Antonoglou, I., Huang, A., Guez, A., Hubert, T., Baker, L., Lai, M., Bolton, A., *et al.*: Mastering the game of go without human knowledge. *nature* **550**(7676), 354–359 (2017)
- [2] Mnih, V., Kavukcuoglu, K., Silver, D., Rusu, A.A., Veness, J., Bellemare, M.G., Graves, A., Riedmiller, M., Fidjeland, A.K., Ostrovski, G., *et al.*: Human-level control through deep reinforcement learning. *nature* **518**(7540), 529–533 (2015)
- [3] Lillicrap, T.P., Hunt, J.J., Pritzel, A., Heess, N., Erez, T., Tassa, Y., Silver, D., Wierstra, D.: Continuous control with deep reinforcement learning (2019). <https://arxiv.org/abs/1509.02971>
- [4] Kalashnikov, D., Irpan, A., Pastor, P., Ibarz, J., Herzog, A., Jang, E., Quillen, D., Holly, E., Kalakrishnan, M., Vanhoucke, V., *et al.*: Scalable deep reinforcement learning for vision-based robotic manipulation. In: Conference on Robot Learning, pp. 651–673 (2018). PMLR
- [5] Fujimoto, S., Hoof, H., Meger, D.: Addressing function approximation error in actor-critic methods. In: International Conference on Machine Learning, pp. 1587–1596 (2018). PMLR
- [6] Haarnoja, T., Zhou, A., Abbeel, P., Levine, S.: Soft actor-critic: Off-policy maximum entropy deep reinforcement learning with a stochastic actor. In: International Conference on Machine Learning, pp. 1861–1870 (2018). Pmlr
- [7] Schulman, J., Wolski, F., Dhariwal, P., Radford, A., Klimov, O.: Proximal Policy Optimization Algorithms (2017). <https://arxiv.org/abs/1707.06347>
- [8] Pinto, L., Davidson, J., Sukthankar, R., Gupta, A.: Robust adversarial reinforcement learning. In: International Conference on Machine Learning, pp. 2817–2826 (2017). PMLR
- [9] Tessler, C., Efroni, Y., Mannor, S.: Action robust reinforcement learning and applications in continuous control. In: International Conference on Machine Learning, pp. 6215–6224 (2019). PMLR
- [10] Long, J., Yu, W., Li, Q., Wang, Z., Lin, D., Pang, J.: Learning H-Infinity Locomotion Control (2024). <https://arxiv.org/abs/2404.14405>
- [11] Silver, D., Lever, G., Heess, N., Degris, T., Wierstra, D., Riedmiller, M.: Deterministic policy gradient algorithms. In: International Conference on Machine Learning, pp. 387–395 (2014). Pmlr
- [12] Basar, T.: A dynamic games approach to controller design: Disturbance rejection in discrete time. In: Proceedings of the 28th IEEE Conference on Decision and

Control,, pp. 407–414 (1989). IEEE

- [13] Stoerwogel, A.A., Weeren, A.J.: The discrete-time riccati equation related to the $h_{\text{sub}}/\text{spl infin}/\text{control}$ problem. *IEEE Transactions on Automatic Control* **39**(3), 686–691 (2002)
- [14] Huang, J., Lin, C.-F.: Numerical approach to computing nonlinear h -infinity control laws. *Journal of Guidance, Control, and Dynamics* **18**(5), 989–994 (1995)
- [15] Başar, T., Bernhard, P.: *H-infinity Optimal Control and Related Minimax Design Problems: a Dynamic Game Approach*. Springer, Boston (2008)
- [16] Rigatos, G., Siano, P., Wira, P., Profumo, F.: Nonlinear h -infinity feedback control for asynchronous motors of electric trains. *Intelligent Industrial Systems* **1**, 85–98 (2015)
- [17] Modares, H., Lewis, F.L., Sistani, M.-B.N.: Online solution of nonquadratic two-player zero-sum games arising in the h -infinity control of constrained input systems. *International Journal of Adaptive Control and Signal Processing* **28**(3-5), 232–254 (2014)
- [18] Al-Tamimi, A., Lewis, F.L., Abu-Khalaf, M.: Model-free q-learning designs for linear discrete-time zero-sum games with application to h -infinity control. *Automatica* **43**(3), 473–481 (2007)
- [19] Deshpande, A.M., Minai, A.A., Kumar, M.: Robust deep reinforcement learning for quadcopter control. *IFAC-PapersOnLine* **54**(20), 90–95 (2021)
- [20] Panerati, J., Zheng, H., Zhou, S., Xu, J., Prorok, A., Schoellig, A.P.: Learning to fly—a gym environment with pybullet physics for reinforcement learning of multi-agent quadcopter control. In: *2021 IEEE/RSJ International Conference on Intelligent Robots and Systems (IROS)*, pp. 7512–7519 (2021). IEEE